

## Dimensional-Crossover-Driven Metal-Insulator Transition in SrVO<sub>3</sub> Ultrathin Films

K. Yoshimatsu,<sup>1</sup> T. Okabe,<sup>1</sup> H. Kumigashira,<sup>1,2,3,\*</sup> S. Okamoto,<sup>4</sup> S. Aizaki,<sup>5</sup> A. Fujimori,<sup>5</sup> and M. Oshima<sup>1,3,6</sup>

<sup>1</sup>Department of Applied Chemistry, University of Tokyo, Bunkyo-ku, Tokyo 113-8656, Japan

<sup>2</sup>PRESTO, Japan Science and Technology Agency, Kawaguchi, Saitama 332-0012, Japan

<sup>3</sup>Synchrotron Radiation Research Organization, The University of Tokyo, Bunkyo-ku, Tokyo 113-8656, Japan

<sup>4</sup>Oak Ridge National Laboratory, Oak Ridge Tennessee 37831-6071, USA

<sup>5</sup>Department of Physics, University of Tokyo, Bunkyo-ku, Tokyo 113-8656, Japan

<sup>6</sup>CREST, Japan Science and Technology Agency, Bunkyo-ku, Tokyo 113-8656, Japan

(Received 12 November 2009; published 9 April 2010)

We have investigated the changes occurring in the electronic structure of digitally controlled SrVO<sub>3</sub> ultrathin films across the metal-insulator transition (MIT) by the film thickness using *in situ* photoemission spectroscopy. With decreasing film thickness, a pseudogap is formed at  $E_F$  through spectral weight transfer from the coherent part to the incoherent part. The pseudogap finally evolves into an energy gap that is indicative of the MIT in a SrVO<sub>3</sub> ultrathin film. The observed spectral behavior is reproduced by layer dynamical-mean-field-theory calculations, and it indicates that the observed MIT is caused by the reduction in the bandwidth due to the dimensional crossover.

DOI: 10.1103/PhysRevLett.104.147601

PACS numbers: 79.60.Jv, 71.30.+h, 73.20.-r

The metal-insulator transition (MIT) is one of the most fundamental phenomena in condensed matter physics [1]. According to the Mott-Hubbard theory [2,3], MIT can be controlled by varying the relative magnitudes of the on-site Coulomb repulsion  $U$  and bandwidth  $W$ . Thus, in the case of bulk materials, MIT has been intensively studied by chemical substitution of constituent ions with ones having a smaller ion radius, where  $W$  is controlled by the resultant changes in the bond angle between transition metal ions and oxygen ions [1]. However, such chemical substitutions always induce randomness in a solid. Further, the unavoidable chemical disorder effects in strongly correlated materials also drive MIT [4,5]. In such a situation, it is not possible to experimentally discriminate between the effects due to changes in  $W$  and those due to disorder in MIT. Consequently, this inability has considerably obscured an exact understanding of MIT induced by bandwidth control.

Here, we propose an alternative approach to understand bandwidth-controlled MIT, using dimensional crossover occurring in an artificial structure. Since a decrease in the layer thickness of ultrathin films causes a reduction in the effective coordination number of constituent ions at the interface and surface, the resultant reduction of the effective  $W$  from a three-dimensional (3D) thick film to the two-dimensional (2D) ultrathin film may drive MIT in the conductive transition metal oxides. The decrease in the layer thickness changes only the bandwidth without causing any chemical fluctuation or disorder concomitant with chemical substitution, and consequently, provides exact information on the bandwidth-controlled MIT.

In this Letter, we have applied this approach to a typical perovskite material with  $3d^1$  configuration, SrVO<sub>3</sub> (SVO). An SVO ultrathin film is an ideal system for studying the dimensional-crossover-driven MIT. This is because of the

robust metallic states in SVO, irrespective of chemical substitutions; SVO with Ca substitution ( $\text{Ca}_{1-x}\text{Sr}_x\text{VO}_3$ ) remains metallic in the entire  $x$  range, in which the bond angle V-O-V is changed from 180° to 160° [6]. By using a digitally controlled film form, we observed the occurrence of MIT induced by the dimensional crossover in SVO ultrathin films by employing *in situ* photoemission spectroscopy (PES). The PES spectra exhibited remarkable and systematic changes as a function of the SVO film thickness. (1) The  $V\ 3d$  derived states near the Fermi level ( $E_F$ ) remain almost unchanged down to 6–8 monolayer (ML), and consist of the coherent part (quasiparticle peak) located at  $E_F$  and the incoherent part (corresponding to the lower Hubbard band) located at 1–2 eV below  $E_F$ . (2) In the case of films having a thickness of 3–6 ML, a pseudogap is formed at  $E_F$  owing to the spectral weight transfer from the coherent part to the incoherent part. (3) The pseudogap finally evolves into an energy gap when the film thickness is reduced to be less than 2 ML, indicating the occurrence of MIT at a critical thickness of 2–3 ML. We compare these experimental results with those obtained using dynamical mean-field theory (DMFT) calculations and discuss the origin of the observed thickness-dependent MIT in terms of the changes occurring in  $W$  due to the dimensional crossover.

Digitally controlled SVO ultrathin films were grown onto atomically flat TiO<sub>2</sub>-terminated 0.05 wt% Nb-doped SrTiO<sub>3</sub> (Nb:STO) substrates in a laser molecular-beam epitaxy chamber connected to a photoemission system at BL2C of the Photon Factory, KEK [7]. During deposition, the substrate temperature was kept at 900 °C under an ultrahigh vacuum of 10<sup>-8</sup> Torr. During the growth of an SVO film, the film thickness was controlled on the atomic scale by monitoring the intensity oscillation of the specular spot observed in reflection high-energy electron diffraction

as shown in Fig. 1(a). The period of oscillation corresponds to the deposition of 1-ML-thick SVO film, which was also confirmed by carefully calibrating the thickness of a thick 100-ML SVO film by grazing-incidence x-ray reflectivity and cross-sectional transmission electron microscopy (TEM). The prepared films were transferred under an ultra-high vacuum of  $10^{-10}$  Torr to the PES chamber. The in-vacuum transfer was necessary to avoid the degradation of the SVO surface on exposure to air [8]. PES spectra were recorded using an SES-100 electron energy analyzer with a total energy resolution of 150 meV. The Fermi level of the samples was referred to that of gold. The surface morphologies and crystal structures of the films were characterized by atomic force microscopy (AFM) and four-circle x-ray diffraction, respectively.

Before discussing the PES spectra, we provide evidence for the fact that the prepared SVO films had atomically flat surfaces and chemically abrupt SVO/Nb:STO interfaces. These features comprise a precondition to the present study, and the evidence guarantees that the precondition is fulfilled. Figures 1(b)–1(d) show the characterizations of an SVO thick film (100 ML). As shown in this figure, atomically flat step-and-terrace structures are observed in the AFM image [Fig. 1(a) and 1(b)], and a chemically abrupt interface is observed in the TEM image [Fig. 1(c)], indicating that the atomic step-and-terrace structure of a growing SVO film is maintained at the film surface and interface while the film grows to a thickness of hundreds of monolayers. In addition, the TEM measurement confirmed the coherent growth of SVO onto Nb:STO substrates without the formation of any dislocations in SVO. The coherent growth of an SVO thin film is also confirmed by the four-circle x-ray diffraction measurement [Fig. 1(d)]. These results suggest that there are no detectable structural disorders in SVO ultrathin films grown on

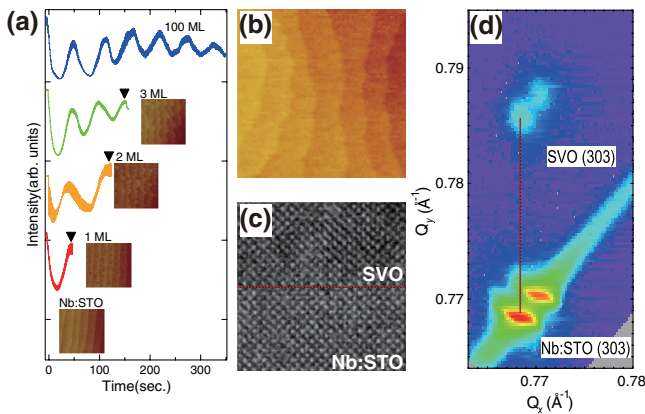


FIG. 1 (color online). Characterizations of  $\text{SrVO}_3$  films grown onto Nb:SrTiO<sub>3</sub> substrates: (a) typical reflection high-energy x-ray diffraction intensity oscillations along with marks where PES spectra were taken and corresponding AFM images (scan area  $0.5 \times 0.5 \mu\text{m}^2$ ). (b) A typical AFM image of SVO (100ML), (c) cross-sectional TEM image of the interface between SVO and Nb:STO, and (d) reciprocal space mapping around the (303) reflection of SVO.

Nb:STO, and the changes in the electronic structure of these films mainly reflect the dimensional-crossover effects.

Figure 2 shows the valence band spectra of SVO ultrathin films grown onto Nb:STO substrates by digitally controlling the SVO layer thickness. These spectra exhibit remarkable and systematic changes. The valence band mainly consists of three structures: two prominent O  $2p$ -derived structures exist at the binding energies of 3.0–9.0 eV [9], whereas a characteristic structure emerges near  $E_F$  of the ultrathin SVO films. The structure near  $E_F$  is assigned to the V  $3d$  states on the basis of V  $2p \rightarrow 3d$  resonant photoemission spectra (not shown). Because the valence band spectrum of Nb:STO exhibits a band gap of 3.2 eV below  $E_F$  owing to the  $n$ -type nature of Nb:STO [10], the V  $3d$  states are well confined in the quantum well structure formed between the vacuum (surface) and the substrate (interface) [11,12]. In the case of thicker SVO films, there are two components attributable to the V  $3d$  states: a peak located precisely at  $E_F$  and a relatively broad peak centered at about 1.5 eV that correspond to the coherent (quasiparticle peak) and incoherent (the remnant of the lower Hubbard band) parts, respectively [9,13]. The intensity of the coherent part is much higher than that of the incoherent part; this feature is similar to that of the bulk spectra reported previously [10,13,14], and confirms that

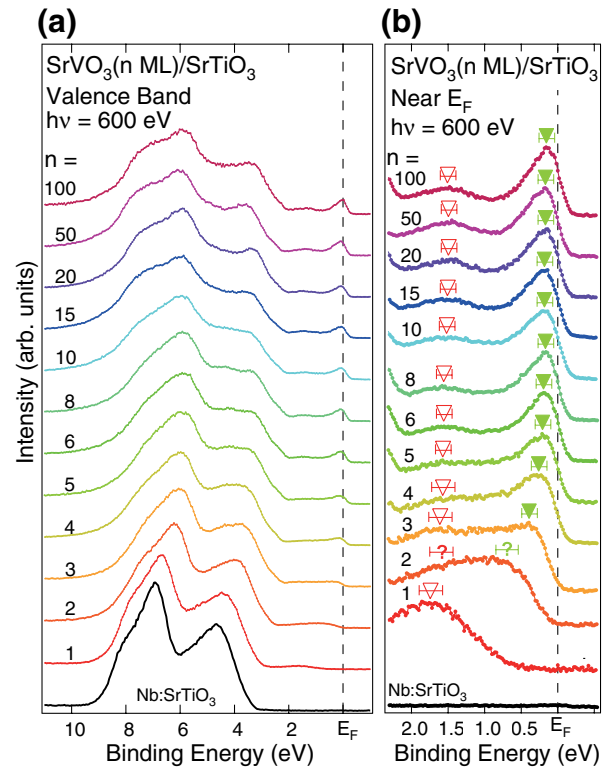


FIG. 2 (color online). (a) *In situ* valence band spectra of  $\text{SrVO}_3$  thin films grown on Nb:SrTiO<sub>3</sub> substrates by digitally controlling the film thickness. (b) PES spectra near  $E_F$ . The filled and open triangles represent the energy positions of the coherent parts and the incoherent parts, respectively.

the SVO thin films prepared in the present study are of high quality.

In order to investigate the changes occurring in the V  $3d$  spectra in more detail, we recorded the near- $E_F$  spectra as shown in Fig. 2(b). The line shapes of these V  $3d$  spectra are almost identical to each other down to a film thickness of 6–8 ML. However, a pseudogap is formed at  $E_F$  when the film layer thickness is reduced to be 3–6 ML; this is because of the spectral weight transfer from the coherent part to the incoherent part. As a result, the centroid of the coherent part gradually departs from  $E_F$  with decreasing layer thickness, and the leading edge of the coherent part clearly shifts below  $E_F$ . With a further decrease in the layer thickness, the V  $3d$  spectra for the film thicknesses of 1–2 ML clearly exhibit the existence of an energy gap at  $E_F$ , whereas small but distinct density of states exist at  $E_F$  when the layer thickness is more than 3 ML, indicating the occurrence of MIT at a critical film thickness between 2 and 3 ML. Finally, the coherent part completely disappears and/or merges into the incoherent part at a layer thickness of 1 ML. On the other hand, the peak position of the incoherent part remains unchanged at about 1.5 eV for the entire range of the film thickness, indicating that  $U$  does not change as a function of the film thickness.

The formation of the energy gap and the pseudogap is further confirmed by the symmetrized V  $3d$  spectra, as shown in Fig. 3(a), where we have subtracted the contribution of the O  $2p$  states from the spectra [13] and symmetrized the obtained spectra with respect to  $E_F$  so as to remove the effects of the Fermi-Dirac function on the spectra [15]. All spectra are normalized to the integrated intensities of the V  $3d$  spectra. For quantitative analysis of the V  $3d$  spectra, we plot the intensity of the coherent part (quasiparticle peak) at  $E_F$  and the peak positions of the coherent and incoherent parts as a function of the SVO film thickness, as shown in Fig. 3(b). The intensity of the coherent part at  $E_F$  is defined as the integrated intensity in the binding-energy range from  $-100$  to  $100$  meV. As expected from Fig. 2(b), within the experimental error, the quasiparticle peak intensity is zero for the SVO film thicknesses of 1 and 2 ML. The intensity steeply increases as the film thickness increases from 2 to 6 ML, which is indicative of the occurrence of MIT at a critical film thickness of 2–3 ML, and the evolution seems to be saturated at a thickness of more than 6 ML. These results suggest that as the layer thickness increases, the bulklike metallic phase is stabilized when the film thickness exceeds 6 ML, after it evolves from the insulator phase present in a film with a thickness of 1–2 ML through the pseudogap region. These behaviors are in good agreement with the evolution of metallic states in Ruddlesden-Popper series of strontium vanadate ( $\text{Sr}_{n+1}\text{V}_n\text{O}_{3n+1}$ ), where a  $\text{SrVO}_3$  layer(s) was (were) sandwiched between SrO insulating block layers: the layered vanadate  $\text{Sr}_2\text{VO}_4$  ( $n = 1$ ) was found to be an insulator, whereas  $\text{Sr}_{n+1}\text{V}_n\text{O}_{3n+1}$  with  $n \geq 2$  exhibited metallic behavior and an increase in conductivity with increasing  $n$  [16–18].

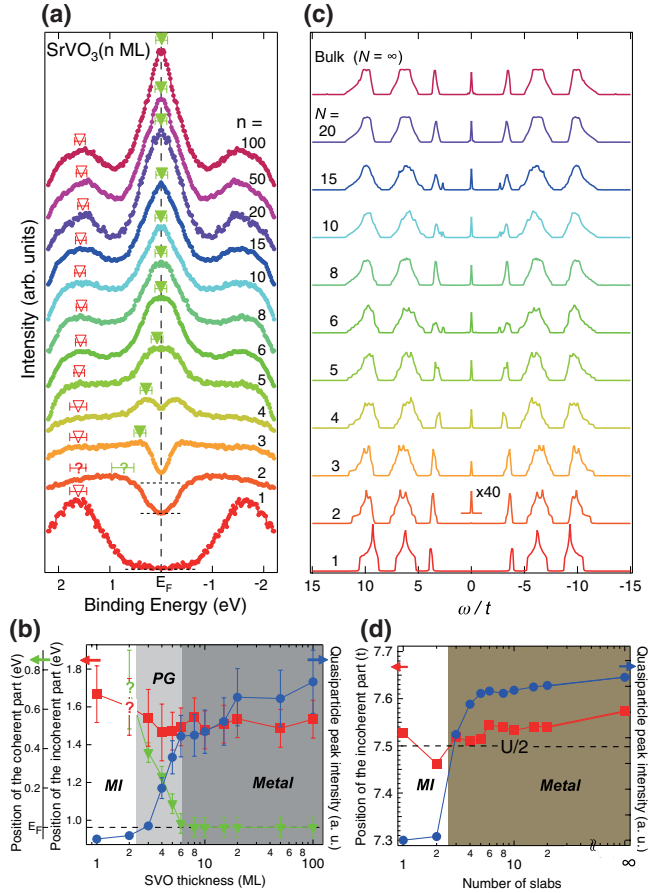


FIG. 3 (color online). (a) Symmetrized V  $3d$  spectra for thickness-dependent  $\text{SrVO}_3$  ultrathin films. The filled and open triangles represent the energy positions of the coherent and incoherent parts, respectively. The dashed lines for 1–3 ML indicate the background level. (b) Plots of the quasiparticle peak intensity and the peak positions of the incoherent and coherent parts in V  $3d$  spectra of SVO ultrathin films as a function of the film thickness. (c) Spectral functions calculated from layer DMFT. (d) Plots of the quasiparticle peak intensity and the centroid of the incoherent part in the calculated spectra as a function of the number of slabs. MI and PG denote the Mott-insulator and pseudogap region, respectively.

The next crucial question is whether the observed thickness-dependent MIT can be understood by dimensional crossover. In order to answer this question, we compare the V  $3d$  spectra with the spectral function obtained from the layer DMFT [19,20]. In this method, the electron self-energy is assumed to be local and depends only on the layer index. The self-energy is fixed by solving the effective impurity model using the exact diagonalization method. In order to make a theoretical model tractable, we consider the multilayered single-band Hubbard model in which slabs are sandwiched between vacuums. This simplicity results in two major discrepancies between the theoretical results and the experimental ones. We discuss the origin of the discrepancies in detail later. For simulating the dimensional-crossover-driven MIT in the calculation, we take the on-site Coulomb repulsion  $U = 15t$  with  $t$

the nearest-neighbor transfer integral. The present single-band Hubbard model shows MIT at  $U = 13t$  in 2D and  $U = 16t$  in 3D by the DMFT. Thus, the system with  $U = 15t$  is insulating in 2D and metallic in 3D, and interpolates the two limits by changing the slab number ( $N$ ) corresponding to the change in the effective bandwidth. The calculated spectral functions are shown in Fig. 3(c), together with the plots of the quasiparticle peak intensity and the centroid of the incoherent part as a function of the slab number [Fig. 3(d)].

As can be seen from the comparison between experimental and theoretical results, the V 3d spectral behavior is reproduced by the DMFT calculations. In the thinnest slabs of  $N = 1$ , the quasiparticle is absent at  $\omega = 0$ , whereas incoherent parts exist in the frequency range from  $-11t$  to  $-3t$  and from  $3t$  to  $11t$  (the lower and upper Hubbard bands, respectively), indicating that  $N = 1$  is a Mott insulator (the three-peak structure is due to the finite-size effect of the impurity solver). In the density of states of  $N \geq 2$ , the quasiparticle peak appears at  $\omega = 0$ . With a further increase in  $N$ , the quasiparticle peak becomes larger and its evolution seems to be saturated at  $N = 6$ , and the spectral function exhibits an almost bulk 3D-like shape. On the other hand, the centroid of the incoherent part (the position of the lower and upper Hubbard bands) remains unchanged at  $7.5t$  (half of  $U$ ) in the entire range of  $N$ . This trend is in good agreement with the experimental results, indicating that the observed thickness-dependent MIT originates from the reduction in the effective bandwidth due to dimensional crossover.

Although the DMFT calculation qualitatively reproduces the layer-dependent V 3d spectra of  $N = 1$  and large  $N$ , there are two discrepancies between the two: (1) the absence of pseudogap formation in the transition region from 3D to 2D and (2) significantly small quasiparticle weight in the theory. These are ascribed to the absence of (a) short-range spatial correlations and (b) orbital degeneracy in the present DMFT. The former is essential for pseudogap formation in low-dimensional systems at a smaller interaction strength than the critical interaction  $U_c$  estimated by the single-site DMFT [21–23]. The real on-site Coulomb repulsion is therefore expected to be smaller than that used in the present calculations. Further, orbital degeneracy ( $N_d$ ) is known to increase  $U_c$  by a factor of about  $\sqrt{N_d}$  [24], resulting in a larger quasiparticle weight in the 3D metallic regime. Here  $N_d = 3$  for the  $t_{2g}$  triplet in the 3D limit, whereas the degeneracy is expected to be lifted ( $N_d < 3$ ) in the 2D regime. Realistic calculations incorporating both the multisite and multi-orbital effects are therefore expected to resolve the above discrepancies. Such calculations are certainly necessary for a quantitative understanding of the observed dimensional crossover but require the development of a better numerical technique.

In conclusion, we have investigated the changes occurring in the electronic structure of digitally controlled

SVO ultrathin films as a function of the layer thickness by *in situ* PES. With decreasing film thickness (decreasing the effective bandwidth due to the dimensional crossover from 3D to 2D), a pseudogap is formed at  $E_F$  owing to the spectral weight transfer from the coherent part to the incoherent part. The pseudogap finally evolves into an energy gap, indicating the dimensional-crossover-driven MIT in an SVO ultrathin film. The layer DMFT yields the correct trend of the observed spectral behavior, except for the pseudogap formation at an intermediate value of  $N$  and a smaller quasiparticle weight in the heavily metallic regime. These discrepancies are ascribed to the multisite and multi-orbital effects which require going beyond the DMFT treatment currently available.

This work was supported by a Grant-in-Aid for Scientific Research (Grants No. A19684010 and No. A19204037) from the Japan Society for the Promotion of Science (JSPS) and JST PRESTO program. K. Y. acknowledges the financial support from JSPS. The work at Oak Ridge National Laboratory was supported by the Division of Materials Sciences and Engineering, Office of Basic Energy Sciences, U.S. Department of Energy.

---

\*kumigashira@sr.t.u-tokyo.ac.jp

- [1] M. Imada, A. Fujimori, and Y. Tokura, *Rev. Mod. Phys.* **70**, 1039 (1998).
- [2] J. Hubbard, *Proc. R. Soc. A* **276**, 238 (1963).
- [3] A. Georges, G. Kotliar, W. Krauth, and M. J. Rozenberg, *Rev. Mod. Phys.* **68**, 13 (1996).
- [4] D. D. Sarma *et al.*, *Phys. Rev. B* **49**, 14238 (1994).
- [5] M. Kobayashi *et al.*, *Phys. Rev. Lett.* **98**, 246401 (2007).
- [6] I. H. Inoue *et al.*, *Phys. Rev. B* **58**, 4372 (1998).
- [7] K. Yoshimatsu, R. Yasuhara, H. Kumigashira, and M. Oshima, *Phys. Rev. Lett.* **101**, 026802 (2008).
- [8] D. H. Kim *et al.*, *Solid State Commun.* **114**, 473 (2000).
- [9] M. Takizawa *et al.*, *Phys. Rev. B* **80**, 235104 (2009).
- [10] V. E. Henrich, G. Dresselhaus, and H. J. Zeiger, *Phys. Rev. B* **17**, 4908 (1978).
- [11] N. V. Smith, *Phys. Rev. B* **32**, 3549 (1985).
- [12] Y. J. Chang *et al.*, *Phys. Rev. Lett.* **103**, 057201 (2009).
- [13] A. Sekiyama *et al.*, *Phys. Rev. Lett.* **93**, 156402 (2004).
- [14] K. Maiti *et al.*, *Phys. Rev. B* **73**, 052508 (2006).
- [15] A. Kanigel *et al.*, *Nature Phys.* **2**, 447 (2006).
- [16] A. Nozaki *et al.*, *Phys. Rev. B* **43**, 181 (1991).
- [17] J. -G. Lee *et al.*, *J. Solid State Chem.* **118**, 292 (1995).
- [18] N. Ohashi *et al.*, *J. Solid State Chem.* **97**, 434 (1992).
- [19] M. Potthoff and W. Nolting, *Phys. Rev. B* **59**, 2549 (1999).
- [20] S. Okamoto and A. J. Millis, *Phys. Rev. B* **70**, 241104 (2004).
- [21] A. Macridin *et al.*, *Phys. Rev. Lett.* **97**, 036401 (2006).
- [22] M. Cavelli *et al.*, *Phys. Rev. Lett.* **95**, 106402 (2005).
- [23] B. Kyung *et al.*, *Phys. Rev. B* **73**, 165114 (2006).
- [24] O. Gunnarsson, E. Koch, and R. M. Martin, *Phys. Rev. B* **54**, R11026 (1996).